

Structural Differences in the DNA Binding Domains of Human p53 and Its *C. elegans* Ortholog Cep-1

Yentram Huyen,^{1,2} Philip D. Jeffrey,⁴
W. Brent Derry,^{6,7} Joel H. Rothman,⁶
Nikola P. Pavletich,^{4,5,*} Elena S. Stavridi,^{1,*}
and Thanos D. Halazonetis^{1,3}

¹Wistar Institute

Philadelphia, Pennsylvania 19104

²Cell and Molecular Biology Program
Biomedical Graduate Studies

³Department of Pathology and Laboratory Medicine
University of Pennsylvania

Philadelphia, Pennsylvania 19104

⁴Cellular Biochemistry and Biophysics Program
Memorial Sloan-Kettering Cancer Center

⁵Howard Hughes Medical Institute
New York, New York 10021

⁶Department of Molecular, Cellular, and
Developmental Biology

Neuroscience Research Institute

University of California, Santa Barbara

Santa Barbara, California 93106

Summary

The DNA binding domains of human p53 and Cep-1, its *C. elegans* ortholog, recognize essentially identical DNA sequences despite poor sequence similarity. We solved the three-dimensional structure of the Cep-1 DNA binding domain in the absence of DNA and compared it to that of human p53. The two domains have similar overall folds. However, three loops, involved in DNA and Zn binding in human p53, contain small α helices in Cep-1. The α helix in loop L3 of Cep-1 orients the side chains of two conserved arginines toward DNA; in human p53, both arginines are mutation hot-spots, but only one contacts DNA. The α helix in loop L1 of Cep-1 repositions the entire loop, making it unlikely for residues of this loop to contact bases in the major groove of DNA, as occurs in human p53. Thus, during evolution there have been considerable changes in the structure of the p53 DNA binding domain.

Introduction

The p53 tumor suppressor protein is a sequence-specific DNA binding transcription factor that induces cell cycle arrest or apoptosis in response to DNA damage (Vogelstein et al., 2000). In more than half of all human tumors, p53 function is inactivated by missense mutations that target its sequence-specific DNA binding domain (Hollstein et al., 1991). The sequence-specific DNA binding domain of p53 has high sequence similarity to the DNA binding domains of p63 and p73, two other

members of the p53 family in humans (Kaghad et al., 1997; Schmale and Bamberger, 1997). All three proteins are thought to have arisen from a common ancestor that may be related to Cep-1 (*Caenorhabditis elegans* p53-related 1), one of the earliest known members of the p53 family in evolution (Derry et al., 2001; Schumacher et al., 2001; Brodsky et al., 2000; Mendoza et al., 2003). Cep-1 is required for the apoptotic response of *C. elegans* germ cells to DNA damage and can activate transcription from reporter plasmids containing human p53 binding sites (Derry et al., 2001; Schumacher et al., 2001). This suggests that Cep-1 and human p53 have similar DNA binding specificities, even though the amino acid sequence identity between the Cep-1 and human p53 DNA binding domains is only 15%. To identify structural features that have been conserved in evolution in the p53 family, we solved the three-dimensional structure of the Cep-1 DNA binding domain and compared it to the practically identical structures of human and mouse p53 DNA binding domains (Cho et al., 1994; Zhao et al., 2001). Unexpectedly, we found that certain structural features of human p53 that are important for sequence-specific DNA binding are not conserved in Cep-1.

Results

Alignment of the amino acid sequences of Cep-1 and human p53 suggests that the DNA binding domain of Cep-1 is located between residues 205 and 425 of the full-length protein. However, due to poor sequence similarity, the precise boundaries of the domain could not be determined. We expressed and purified recombinant proteins corresponding to residues 205–425, 216–420, and 220–420 of Cep-1 and screened them for their ability to crystallize. The protein spanning residues 220–420 formed crystals that diffracted to 2 Å resolution. Phases were calculated using a mercury derivative, and a structure was solved in which residues 223–418 of Cep-1 are well defined (Table 1). We also attempted to obtain crystals of Cep-1 bound to DNA; however, these efforts were not successful.

Cep-1 adopts a β sandwich fold and contains key structural elements present in human and mouse p53, such as the Zn binding site, helix H2 that contacts the major groove of DNA, and the β hairpin that lies between helix H2 and the β sandwich (Figures 1A and 1B). However, there are also interesting differences. First, the N-terminal end of the Cep-1 DNA binding domain is just N-terminal to strand S1, whereas human p53 has a coil N-terminal to strand S1 that packs against several of the strands that form the β sandwich. The second difference relates to loops L1, L2, and L3, which in human p53 are involved in DNA and Zn binding. In human p53, these loops do not contain secondary structure, but in Cep-1, each of the loops contains a small segment that adopts an α -helical conformation. We refer to the α helices within loops L1, L2, and L3 as helices Ha, Hb, and Hc, respectively.

*Correspondence: nikola@xray2.mskcc.org (N.P.P.), stavridi@wistar.upenn.edu (E.S.S.)

⁷Present address: The Hospital for Sick Children, University of Toronto, Toronto, Ontario, Canada M5G 1X8.

Table 1. Data Collection and Refinement Statistics

Data Collection		
Data set	Native	Mercury chloride
Space Group	P2 ₁ 2 ₁ 2 ₁	P2 ₁ 2 ₁ 2 ₁
Resolution (Å)	2.0	2.0
Observations	229,657	239,994
Unique reflections	16,384	16,454
Data coverage (%)	99.2	99.3
R _{sym} (%)	8.8	11.5
Phasing Analysis (20.0–2.0 Å)		
Phasing power (centric)	—	1.26
Phasing power (acentric)	—	1.44
R _{cullis} (centric)	—	0.63
R _{cullis} (acentric)	—	0.74
Refinement Statistics		
Resolution range (Å)	15.0–2.1	
Reflections used (>0 sigF)	14,247	
Protein atoms	1,651	
Zn atoms	1	
Water molecules	155	
R factor (%)	17.6	
R _{free} (%)	23.4	
Rms deviations		
Bonds (Å)	0.010	
Angles (°)	1.53	
Ramachandran plot		
Most favored (%)	90.8	
Allowed (%)	9.2	

$R_{sym} = \sum_n \sum_i |I_{h,j} - I_n| / \sum_n \sum_i I_{h,j}$ for the intensity (I) of i observations of reflection h . Phasing power = $\langle F_{ph} \rangle / E$, where $\langle F_{ph} \rangle$ is the root-mean-square heavy atom structure factor and E is the residual lack of closure error. $R_{cullis} = \text{mean residual lack of closure error divided by the dispersive difference}$. R factor = $\sum |F_{obs} - F_{calc}| / \sum |F_{obs}|$, where F_{obs} and F_{calc} are the observed and calculated structure factors, respectively. R_{free} = R factor calculated using 5% of the reflection data chosen randomly and omitted from the start of refinement. Rms deviations for bonds and angles are the respective root-mean-square deviations from ideal values.

The secondary structure elements of Cep-1 are shown in Figure 1C, which also shows a structure-based alignment of the amino acid sequences of the DNA binding domains of human p53 and Cep-1. Practically all the residues that are identical in human p53 and Cep-1 map to parts of the structure where the human p53 and Cep-1 backbones overlay well when the two structures are superimposed (Figure 1C; identical residues are indicated by vertical lines, residues whose C α atoms are within 3.0 Å in the superimposed Cep-1 and human p53 structures are colored red). Interestingly, there were two exceptions to this general observation. Within loops L1 and L3, there were residues that are conserved in evolution but do not overlay when the structures are superimposed. This is because of the different conformations adopted by loops L1 and L3 in human p53 and Cep-1.

The main difference in the conformation of loop L1 between Cep-1 and human p53 is that in Cep-1 residues 231–236 within the N-terminal half of the loop form helix Ha, whereas in human p53 the entire loop lacks helical secondary structure (Figure 2A). Since the number of amino acids that comprise loop L1 in the two proteins is the same (Figure 2D), the presence of helical secondary structure only in Cep-1 leads to the tip of loop L1 adopt-

ing different positions in the two proteins. In human p53, the tip extends as far forward as helix H2, allowing Lys120, the residue at the L1 tip, to contact a base in the major groove of DNA (Figures 2A, 2C, and 3C). In Cep-1, the corresponding residue, Lys237, is recessed relative to helix H2 and appears unable to contact a base in the major groove of DNA. The difference in the position of human p53 Lys120 and Cep-1 Lys237 contrasts with the fact that this lysine is invariant throughout evolution in p53, p63, and p73 proteins, and even in amoeba p53 (Figure 2D). Further, with few exceptions, the two residues that surround this lysine (Ala236 and Ser238 in Cep-1; Ala119 and Ser121 in human p53) are also invariant in evolution (Kaghad et al., 1997; Schmale and Bamberger, 1997; Derry et al., 2001; Schumacher et al., 2001; Brodsky et al., 2000; Mendoza et al., 2003).

We examined the importance of Lys237 for DNA binding using in vitro translated Cep-1 proteins in an electrophoretic mobility shift assay. Our prior experience with human p53 suggests that in this assay DNA binding requires p53 to be in its native oligomeric form (Waterman et al., 1995). We therefore fused the DNA binding domain of Cep-1 (residues 220–420), which by gel filtration analysis behaves as a monomer, to a C-terminal fragment of human p53 (residues 309–393) that contains the tetramerization domain and the epitope for antibody PAb421. This fusion protein bound an oligonucleotide containing the p53 target site present in the promoter of the *cip1/waf1/p21* gene (El-Deiry et al., 1993), and the protein-DNA complex was supershifted with antibody PAb421, confirming that it contained the Cep-1 fusion protein (Figure 2E). Substitution of Lys237 with alanine clearly compromised DNA binding (Figure 2F). Since both the wild-type and mutant Cep-1 fusion proteins were expressed at similar levels (Figure 2G), we conclude that Lys237 is important for DNA binding.

The C-terminal half of loop L3 also adopts distinct conformations in Cep-1 and human p53; in Cep-1 it is α -helical (helix Hc), while in human p53 it has no helical secondary structure (Figures 2A and 2B). In human p53, this region contains two residues that are mutation hot-spots in cancer: Arg248, which contacts the minor groove of DNA, and Arg249, which stabilizes the native structure of loops L2 and L3 by forming a salt bridge with Glu171 from loop L2 (Figure 2A). Both these arginines are very highly conserved in evolution (Figure 2D). For Arg248, this would be expected, since this residue contacts DNA; for Arg249, the evolutionary conservation is harder to explain, since structural residues are typically not so highly conserved through evolution. Arg248 and Arg249 of human p53 correspond to Arg371 and Arg372 of Cep-1, respectively. Arg371 adopts a conformation similar to that of Arg248 of human p53. However, the side chain of Arg372 does not point toward loop L2, as does the side chain of Arg249 of human p53, but rather it points in the same direction as the side chain of Arg371 (Figures 2A and 2B). This suggested that Arg372 may contact DNA, and indeed, substitution of Arg372 with alanine rendered Cep-1 incapable of binding DNA (Figures 2F and 2G).

The ability of Cep-1 to bind to the p53 target site in the promoter of the human *cip1/waf1/p21* gene (Figure 2E) (Schumacher et al., 2001) indicates that Cep-1 and

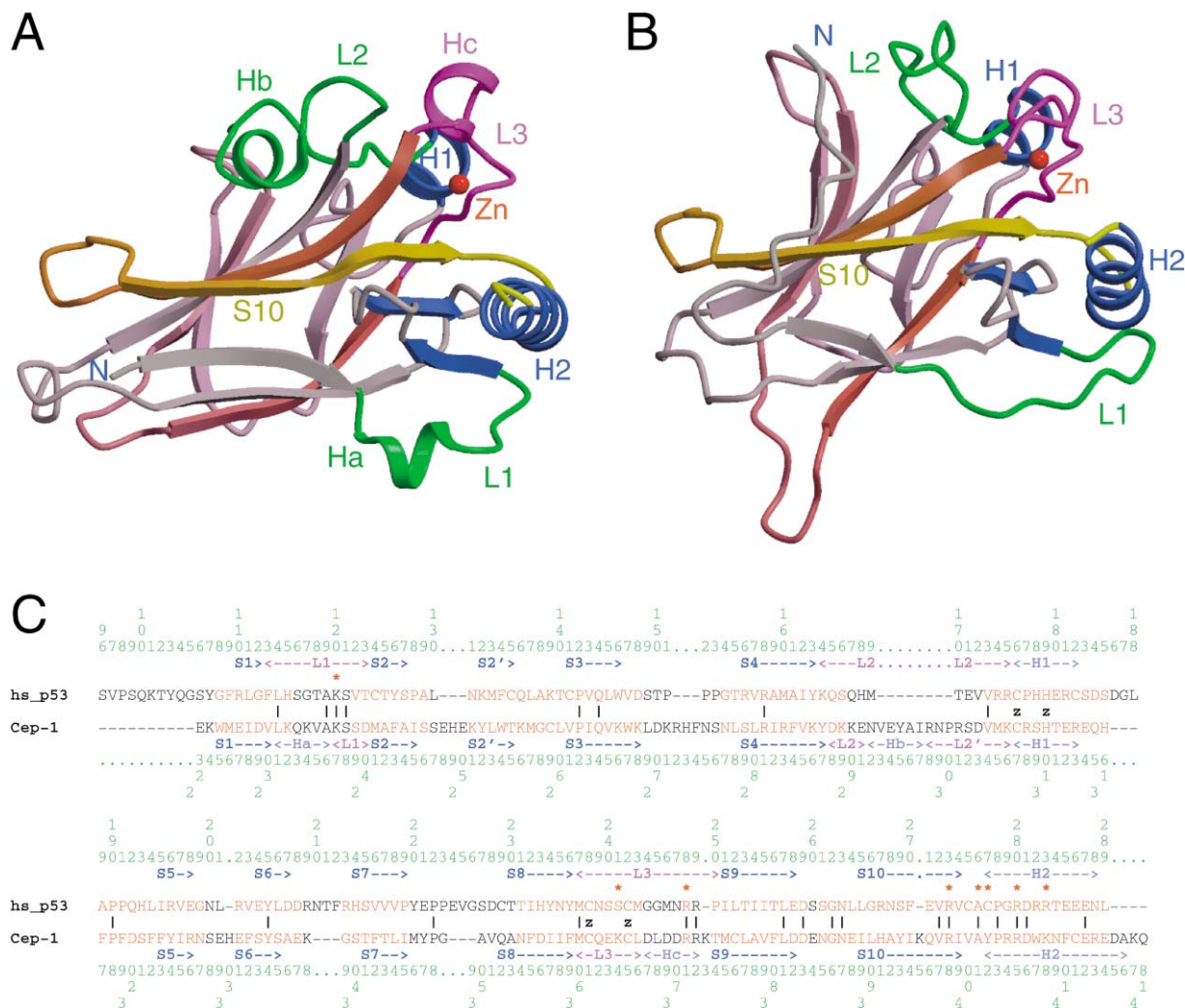


Figure 1. Structure of Cep-1 DNA Binding Domain and Comparison to Human p53

(A and B) Ribbons representation of the Cep-1 (A) and human p53 (B) DNA binding domains shown in the same orientation. In the human p53 structure (PDB ID 1TSR, chain B), helix H2 and the tip of loop L1 bind to the major groove of DNA, which is not shown in this figure. Select secondary structure elements are labeled H1, H2, Ha, Hb, and Hc (α helices), L1, L2, and L3 (loops), and S10 (β strand). N, N terminus. (C) Structure-based alignment of the sequences of Cep-1 and human p53 (hs_p53) DNA binding domains. Residues whose C α atoms are within 3.0 Å in the superimposed Cep-1 and human p53 structures are colored red. The numbering refers to codon positions of human p53 (above the aligned sequences) and Cep-1 (below the aligned sequences). Vertical lines, residues that are identical in human p53 and Cep-1; z, residues that coordinate Zn; asterisks, residues of human p53 that contact DNA.

human p53 have similar DNA binding specificities. The optimal binding site for human p53 contains four nearly identical tandem copies of the pentamer repeat sequence G-G-Pu-C-A (Pu, purine) arranged in a head-to-tail orientation (Figure 3A) (El-Deiry et al., 1992; Halazonetis et al., 1993). We compared more carefully the DNA binding specificities of Cep-1 and human p53 using oligonucleotides that differ from the optimal human p53 binding site by having the same single nucleotide substitution in each of the four pentamer repeats. Like human p53, Cep-1 shows preference for purine at positions 5 and 3 of the repeat, requires cytosine at position 2, and shows preference for adenine at position 1. The only difference in DNA binding specificity related to position 4. Human p53 has equal preference for A and G, lower preference for T, and no affinity for C, whereas Cep-1

has highest preference for A, lower preference for G and C and no affinity for T (Figure 3B).

The high similarity in DNA binding sequence specificity between Cep-1 and human p53 suggested that the residues of human p53 that contact DNA would be conserved in Cep-1. In human p53, three residues contact DNA bases: Lys120, Cys277, and Arg280 (Figures 3A and 3C) (Cho et al., 1994). Arg280 in helix H2 contacts the invariant guanine at position 2' of the pentamer repeat. The corresponding residue in Cep-1, Arg405, is expected to make a similar DNA contact. Cys277 of human p53 contacts the cytosine at position 3' of the pentamer repeat; the equivalent residue in Cep-1, Y402, has a much bulkier side chain, raising concerns as to whether it can make a similar DNA contact. Finally, Lys120 in loop L1 of human p53 contacts the guanine

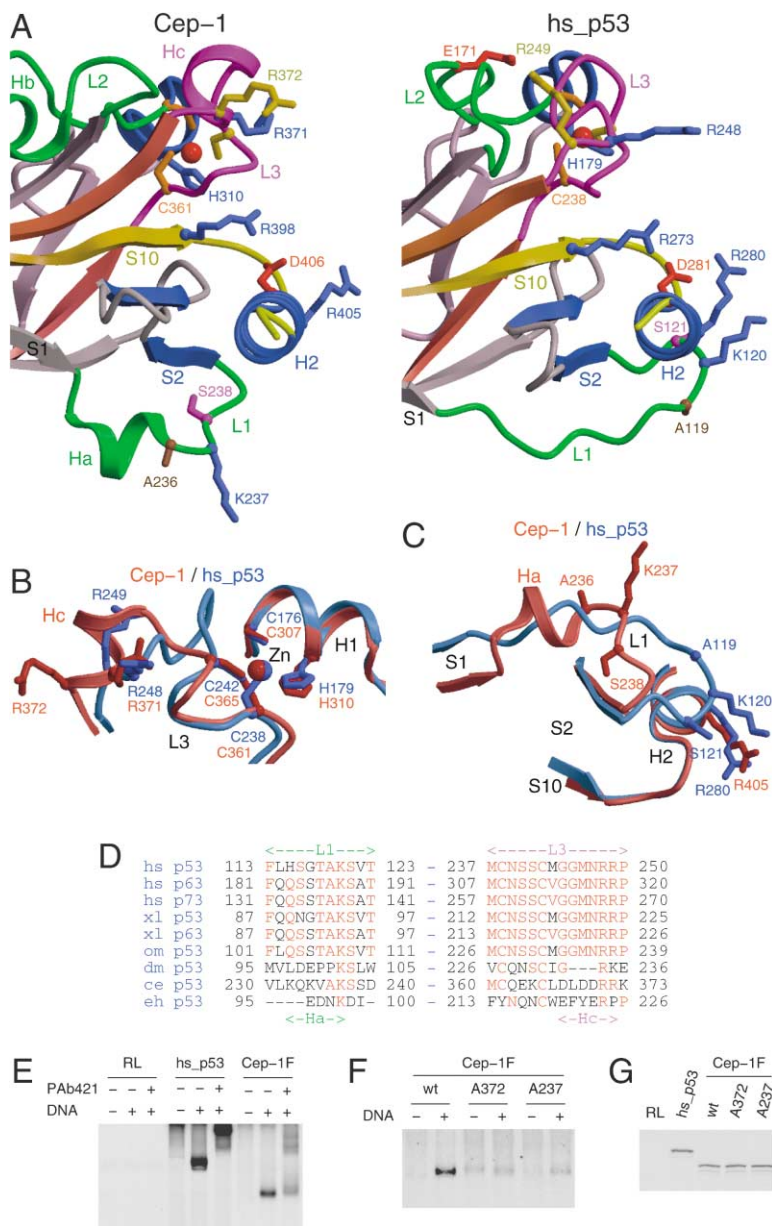


Figure 2. Comparison of the Loop L1 and L3 Structures of Cep-1 and Human p53

(A) Structure of loops L1 and L3 and adjacent elements of Cep-1 and human p53 (hs_p53) viewed in approximately the same orientation as shown in Figure 1.

(B) Superimposition of Cep-1 and human p53 on the basis of the C α atoms of the residues that chelate Zn to show the different conformations of loop L3 in the two proteins. The views in (A) and (B) are related to each other by a 90 $^\circ$ rotation along the y axis.

(C) Superimposition of Cep-1 and human p53 on the basis of the C α atoms of the residues of helix H2 to show the different conformations of loop L1 in the two proteins. The views in (A) and (C) are related to each other by a 150 $^\circ$ rotation along the x axis. In the human p53 structure (PDB ID 1T5R, chain B), helix H2 and the tip of loop L1 bind to the major groove of DNA, which is not shown in this figure. The side chains of select residues are labeled using the single letter amino acid code and codon number, and select secondary structure elements are marked: loops L1, L2, and L3; α helices H1, H2, Ha, Hb, and Hc; and β strands S1, S2, and S10.

(D) Sequence alignment of the residues comprising loops L1 and L3 in various members of the p53 protein family through evolution. The boundaries for helices Ha and Hc refer to Cep-1. Species are abbreviated as follows: hs, *Homo sapiens*; xl, *Xenopus laevis*; om, *Oncorhynchus mykiss* (trout); dm, *Drosophila melanogaster*; ce, *Caenorhabditis elegans*; eh, *Entamoeba histolytica*.

(E-G) DNA binding activity of Cep-1. (E) Binding of wild-type human p53 (hs_p53) and of a protein containing the Cep-1 DNA binding domain fused to the tetramerization domain and C terminus of human p53 (Cep-1F) to the p53 target site present in the *cip1/waf1/p21* gene. RL, unprogrammed reticulocyte lysate. (F) DNA binding of Cep-1F with a wild-type (wt) Cep-1 DNA binding domain or a Cep-1 DNA binding domain in which Lys237 or Arg372 was substituted with alanine (A237 and A372, respectively). (G) Autoradiogram of the 35 S-labeled in vitro translated human p53 and Cep-1F proteins used in the DNA binding assays. The proteins were resolved by SDS-polyacrylamide gel electrophoresis. RL, unprogrammed reticulocyte lysate.

at position 4 of the repeat. In Cep-1, the equivalent residue, Lys237, adopts a significantly different position because of the different loop L1 conformations in the two proteins (Figures 2C and 3C). This may explain the different binding specificity of Cep-1 and human p53 for position 4 (Figure 3B). Overall, however, it is somewhat surprising that Cep-1 and human p53 have identical DNA binding specificities at four out of five positions of the pentamer repeat, even though only the DNA base contacts mediated by Arg280 of human p53 appear to be conserved in Cep-1.

Discussion

Cep-1 and human p53 have remarkably similar DNA binding specificities, predicting a high degree of three-

dimensional structure conservation. Yet surprisingly, the structure of Cep-1 has several differences from the previously solved human and mouse p53 structures (Cho et al., 1994; Zhao et al., 2001), making it hard to understand how these proteins have such similar DNA binding specificities. The most interesting differences relate to the residues that contact DNA bases and the conformations of loops L1 and L3.

Structural superimposition of the human p53 and Cep-1 DNA binding domains reveals that of the three human p53 residues that contact DNA bases (Lys120, Arg280, and Cys277), only the contacts mediated by Arg280 are likely to be conserved in Cep-1 (Figure 3). This was unexpected given the similar DNA binding specificity. One possible explanation for this finding is that a significant fraction of the DNA binding specificity

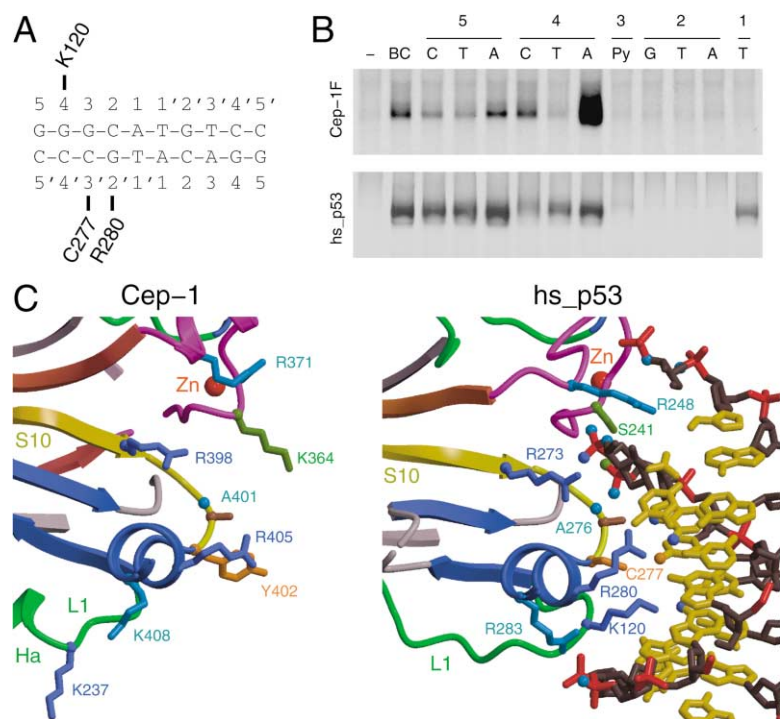


Figure 3. Comparison of the DNA Binding Specificity of Cep-1 and Human p53 and Conservation of DNA Binding Residues of Human p53 in Cep-1

(A) Nucleotide sequence of two of the four tandem inverted pentamer repeats comprising the optimal full-length binding site for human p53. The nucleotides are numbered according to their position in the pentamer. The human p53 residues that contact bases in the first pentamer repeat are indicated next to the nucleotide they contact.

(B) DNA binding specificity of human p53 (hs_p53) and the Cep-1F fusion protein containing the wild-type Cep-1 DNA binding domain fused to the human p53 tetramerization domain and C terminus. Oligonucleotide BC contains the optimal binding site for human p53 shown in (A). Variants of oligonucleotide BC contain one nucleotide substitution in each pentamer repeat; the position of the substitution and the variant nucleotide are indicated. At position 3, the variant has a pyrimidine (Py), instead of purine, such that the sequence of two adjacent pentamer repeats is GGTCATGGCC.

(C) Conservation of DNA binding residues of human p53 in Cep-1. The side chains of the human p53 residues that contact DNA and the corresponding Cep-1 residues are indicated. The atoms of DNA in contact with hu-

man p53 residues have the same color as the side chains of those residues. Ala276 contacts DNA through its amide nitrogen (shown as a light blue sphere on the protein backbone). The side chain of Ala276, colored brown, does not contact DNA.

is contributed by residues that contact the DNA backbone. Several of the human p53 residues that contact the DNA backbone are identical in Cep-1; specifically, human p53 residues Arg248, Arg273, and Ala276 correspond to Cep-1 residues Arg371, Arg398, and Ala401, respectively (Figure 3C). Conservation of the contacts mediated by Arg248 of human p53 could be particularly important, since these contacts are likely to confer DNA binding sequence specificity by requiring compression of the DNA minor groove (Cho et al., 1994).

The second interesting difference relates to loop L3, which adopts different conformations in Cep-1 and human p53 (Figure 2B). The three-dimensional structure difference predicts that evolutionarily conserved residues have different roles in the two p53 proteins. Specifically, Arg249 in loop L3 of human p53 forms a salt bridge with Glu171 that stabilizes the native structure of loop L3 (Figure 2A); in Cep-1, the corresponding Arg372 most likely contacts DNA as predicted by the three-dimensional structure and by the loss of DNA binding activity, when this residue is substituted with alanine (Figure 2F). The change in orientation of the side chain of Cep-1 Arg372 relative to human p53 Arg249 is due to the difference in secondary structure in this region of loop L3; in Cep-1 this region is α -helical, but in human p53 it is random coil.

The most dramatic difference between the structures of Cep-1 and human p53 is undoubtedly the conformation of loop L1. Loop L1 has previously attracted attention because it is a cold spot for mutations in human cancer and because substitutions targeting residues of loop L1 often enhance the affinity of human p53 for specific DNA sequences (Saller et al., 1999; Inga et al.,

2001). An explanation for these observations is not obvious from the structure of the human p53 DNA binding domain, and unfortunately, the structure of Cep-1 does not provide an answer either.

In human p53, loop L1 packs against helix H2, forming a contiguous DNA binding surface that occupies the major groove of DNA (Figure 4A). Given that the lysine at the tip of loop L1 is conserved in Cep-1 and human p53 and that this lysine contributes to DNA binding in both proteins, we had expected that in Cep-1, helix H2 and loop L1 would form a contiguous DNA binding surface similar to the one observed in human p53. However, this was not the case (Figure 4A). It is formally possible that when Cep-1 binds DNA, loop L1 adopts a conformation similar to the one observed in human p53. We think, however, that this is unlikely. There is no precedent for a conformational switch of this magnitude between the free and DNA-bound forms of human p53, which are practically identical to each other (Cho et al., 1994; Zhao et al., 2001). Further, our attempts to model loop L1 of Cep-1 so that it adopts the same backbone conformation as loop L1 of human p53 led to unresolvable steric clashes with Cep-1 helix H2 residues. We therefore favor the model that the DNA-bound form of Cep-1 adopts a conformation very similar to the one observed in the absence of DNA. In this case, Lys237, or any other residue in loop L1, would be unable to contact bases in the major groove of DNA. In fact, Lys237 could not even make a DNA backbone contact if Cep-1 were to bind DNA in exactly the same orientation as human p53 (Figure 4A). However, mutagenesis analysis suggests that Lys237 contributes to Cep-1 DNA binding (Figure 2F). To determine whether the position of

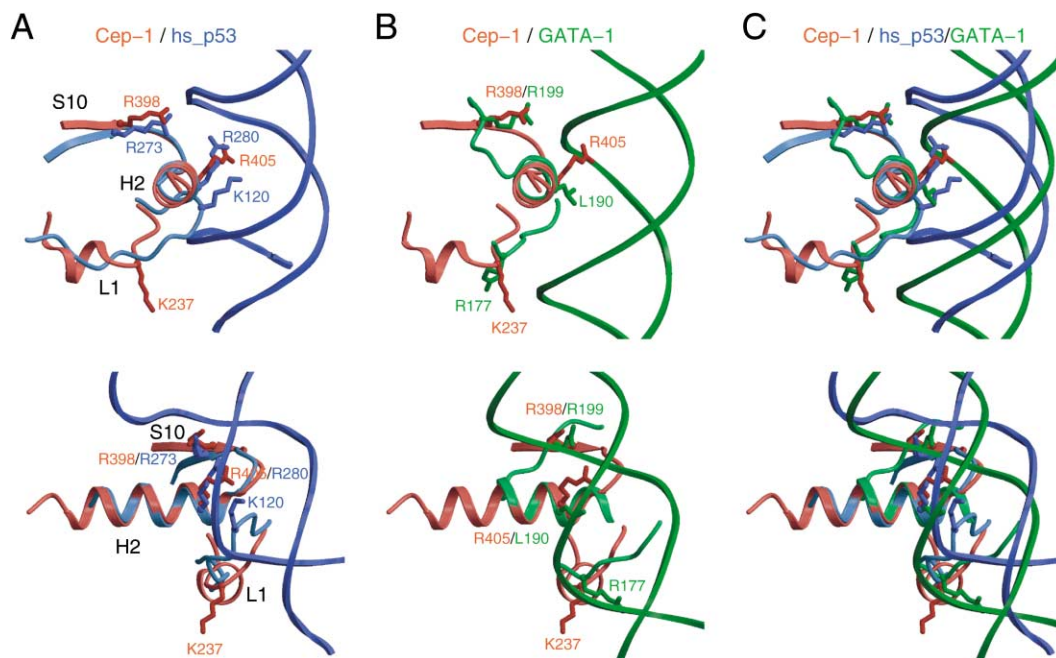


Figure 4. Structural Superimposition of Select Secondary Structure Elements and Residues of Cep-1, Human p53, and the Erythroid Transcription Factor GATA-1

(A) Cep-1 and human p53 (hs_p53). (B) Cep-1 and GATA-1 (PDB ID 2GAT). (C) Cep-1, human p53 and GATA-1. Cep-1 is colored red, human p53 and its bound DNA are colored blue, and GATA-1 and its bound DNA are colored green. The two views are related by a 90° rotation along the y axis, and the orientation in the top panel is similar to that shown in Figure 1. Cep-1 secondary structure elements: S10, strand 10; H2, helix 2; L1, loop L1.

Lys237 is compatible with DNA binding, we structurally superimposed helix H2 and residues Lys237 and Arg398 of Cep-1 with the α helix and residues Arg177 and Arg199 of the chicken erythroid transcription factor GATA-1 (Omichinski et al., 1993). The superimposition was remarkably good (Figure 4B). The α helix of GATA-1 binds to the major groove of DNA, while the side chains of residues Arg177 and Arg199 contact the phosphate backbone. If Cep-1 were to bind DNA like GATA-1, then Cep-1 would adopt the more conventional DNA binding motif of a single α helix in the major groove, and residues Arg398 and Lys237 would contact the phosphate backbone (Figure 4B). In this case, the orientation of bound DNA would differ from that observed in the human p53/DNA complex (Figure 4C), and human p53 and Cep-1 would recognize the major groove of DNA via different motifs: helix-loop for human p53 and helix only for Cep-1.

It is hard to fully reconcile the differences in the three-dimensional structures of Cep-1 and human p53 (residues that contact DNA bases in human p53 are not evolutionarily conserved in Cep-1, and loops L3 and L1 adopt different conformations) with the observation that Cep-1 and human p53 have very similar DNA binding specificities. We are proposing that Cep-1 and human p53 differ in the way they recognize DNA. Yet, a high degree of structural similarity would better explain the conservation in DNA binding specificity. It is probably fair to conclude that our understanding regarding how p53 proteins bind DNA through evolution is as yet incomplete.

Experimental Procedures

Protein Expression and Purification

The Cep-1 DNA binding domain (residues 220–420) was expressed in *E. coli* BL21 cells at 30°C. Cells were lysed in buffer consisting of 25 mM bis-tris propane (BTP) (pH 6.8), 250 mM NaCl, 10 mM DTT, and protease inhibitors, and the polypeptide was purified by cation exchange (Resource S column; Pharmacia) and gel filtration (Superdex 200 column; Pharmacia) chromatography. The protein eluted from the gel filtration column in buffer consisting of 25 mM BTP (pH 6.8), 200 mM NaCl, and 10 mM DTT.

Crystallization and Data Collection

Crystals were grown at room temperature by the hanging drop vapor diffusion method by mixing the protein at 10 mg/ml with an equal volume of reservoir solution containing 0.8–1.1 M sodium citrate, 100 mM BTP (pH 9.2), 5% isopropyl alcohol (IPA), and 10 mM DTT. Crystallization started at day 1, and crystals grew to their final size over a 2–3 day period. The crystals formed in space group P2₁2₁2₁ with dimensions $a = 39.36 \text{ \AA}$, $b = 68.43 \text{ \AA}$, $c = 88.18 \text{ \AA}$, and contained one molecule in the asymmetric unit. Heavy-atom derivatives were obtained by soaking the crystals in harvest buffer (1.2 M sodium citrate, 100 mM BTP [pH 9.2], and 5% IPA) supplemented with 0.5 mM mercury chloride, 1 mM β -mercaptoethanol, and 5%–10% ethylene glycol for 2 hr. All data sets were collected using flash-frozen crystals on a Rigaku R-Axis IV imaging plate area detector mounted on a Rigaku rotating anode X-ray generator. Reflection data were indexed, integrated, and scaled using the programs DENZO and SCALEPACK (Otwinowski and Minor, 1997).

Structure Determination and Refinement

The positions of four mercury atoms were calculated using the program SHELX (Schneider and Sheldrick, 2002). Phases were calculated at 2.0 \AA using the isomorphous signal of the heavy metal atoms with the program MLPHARE (CCP4, 1994). The phases had a mean figure of merit of 0.40 at 3.03 \AA resolution (Table 1). After solvent

flattening using DM (CCP4, 1994), the experimental electron density map showed clear density for all of the backbone and most side chain atoms. An initial model was built with the program ARP/WARP (Morris et al., 2002), improved by several cycles of manual rebuilding with the program O (Jones et al., 1991), and refined with the program CNS (Brünger et al., 1998). Figures were prepared using the programs MOLSCRIPT, BOBSCRIPT, and RASTER3D (Kraulis, 1991; Esnouf, 1997; Merritt and Bacon, 1997).

DNA Binding Assays

DNA binding was performed using in vitro translated proteins as previously described (Halazonetis et al., 1993; Waterman et al., 1995). The sequence of the oligonucleotide containing the p53 target site in *cip1/waf1/p21* is CCC-GAACA-TGTCC-CAACA-TGTTG-GGG; the sequence of oligonucleotide BC is CC-GGGCA-TGTCC-GGGCA-TGTCC-GGGCATGT.

Acknowledgments

The authors thank the Wistar Institute Protein Chemistry and Nucleic Acid Facilities for protein N-terminal sequencing, mass spectrometry analysis, and DNA sequencing analysis. This research was supported in part by grant CA76367 to T.D.H. from the National Cancer Institute.

Received: March 1, 2004

Revised: May 10, 2004

Accepted: May 10, 2004

Published: July 13, 2004

References

- Brodsky, M.H., Nordstrom, W., Tsang, G., Kwan, E., Rubin, G.M., and Abrams, J.M. (2000). Drosophila p53 binds a damage response element at the reaper locus. *Cell* **101**, 103–113.
- Brünger, A.T., Adams, P.D., Clore, G.M., DeLano, W.L., Gros, P., Grosse-Kunstleve, R.W., Jiang, J.S., Kuszewski, J., Nilges, M., Pannu, N.S., et al. (1998). Crystallography and NMR system: a new software suite for macromolecular structure determination. *Acta Crystallogr. D Biol. Crystallogr.* **54**, 905–921.
- CCP4 (Collaborative Computational Project 4) (1994). The CCP4 suite: programs for protein crystallography. *Acta Crystallogr. D Biol. Crystallogr.* **50**, 760–763.
- Cho, Y., Gorina, S., Jeffrey, P.D., and Pavletich, N.P. (1994). Crystal structure of a p53 tumor suppressor-DNA complex: understanding tumorigenic mutations. *Science* **265**, 346–355.
- Derry, W.B., Putzke, A.P., and Rothman, J.H. (2001). *Caenorhabditis elegans* p53: role in apoptosis, meiosis, and stress resistance. *Science* **294**, 591–595.
- El-Deiry, W.S., Kern, S.E., Pietenpol, J.A., Kinzler, K.W., and Vogelstein, B. (1992). Definition of a consensus binding site for p53. *Nat. Genet.* **1**, 45–49.
- El-Deiry, W.S., Tokino, T., Velculescu, V.E., Levy, D.B., Parsons, R., Trent, J.M., Lin, D., Mercer, W.E., Kinzler, K.W., and Vogelstein, B. (1993). WAF1, a potential mediator of p53 tumor suppression. *Cell* **75**, 817–825.
- Esnouf, R.M. (1997). An extensively modified version of Molscript that includes greatly enhanced coloring capabilities. *J. Mol. Graph. Model.* **15**, 132–134.
- Halazonetis, T.D., Davis, L.J., and Kandil, A.N. (1993). Wild-type p53 adopts a 'mutant'-like conformation when bound to DNA. *EMBO J.* **12**, 1021–1028.
- Hollstein, M., Sidransky, D., Vogelstein, B., and Harris, C.C. (1991). p53 mutations in human cancers. *Science* **253**, 49–53.
- Inga, A., Monti, P., Fronza, G., Darden, T., and Resnick, M.A. (2001). p53 mutants exhibiting enhanced transcriptional activation and altered promoter selectivity are revealed using a sensitive, yeast-based functional assay. *Oncogene* **20**, 501–513.
- Jones, T.A., Zou, J.Y., Cowan, S.W., and Kjeldgaard, M. (1991). Improved methods for building protein models in electron density

maps and the location of errors in these models. *Acta Crystallogr. A* **47**, 110–119.

Kaghad, M., Bonnet, H., Yang, A., Creancier, L., Biscan, J.C., Valent, A., Minty, A., Chalon, P., Lelias, J.M., Dumont, X., et al. (1997). Monoallelically expressed gene related to p53 at 1p36, a region frequently deleted in neuroblastoma and other human cancers. *Cell* **90**, 809–819.

Kraulis, P. (1991). Molscript: a program to produce both detailed and schematic plots of protein structures. *J. Appl. Crystallogr.* **24**, 946–950.

Mendoza, L., Orozco, E., Rodriguez, M.A., Garcia-Rivera, G., Sanchez, T., Garcia, E., and Gariglio, P. (2003). Ehp53, an *Entamoeba histolytica* protein, ancestor of the mammalian tumour suppressor p53. *Microbiol.* **149**, 885–893.

Merritt, E.A., and Bacon, D.J. (1997). Raster3D—photorealistic molecular graphics. *Methods Enzymol.* **277**, 505–524.

Morris, R.J., Perrakis, A., and Lamzin, V.S. (2002). ARP/wARP's model-building algorithms. I. The main chain. *Acta Crystallogr. D Biol. Crystallogr.* **58**, 968–975.

Omichinski, J.G., Clore, G.M., Schaad, O., Felsenfeld, G., Trainor, C., Appella, E., Stahl, S.J., and Gronenborn, A.M. (1993). NMR structure of a specific DNA complex of Zn-containing DNA binding domain of GATA-1. *Science* **261**, 438–446.

Otwinowski, Z., and Minor, W. (1997). Processing of X-ray diffraction data collected in oscillation mode. *Methods Enzymol.* **276**, 307–326.

Saller, E., Tom, E., Brunori, M., Otter, M., Estreicher, A., Mack, D.H., and Iggo, R. (1999). Increased apoptosis induction by 121F mutant p53. *EMBO J.* **18**, 4424–4437.

Schmale, H., and Bamberger, C. (1997). A novel protein with strong homology to the tumor suppressor p53. *Oncogene* **15**, 1363–1367.

Schneider, T.R., and Sheldrick, G.M. (2002). Substructure solution with SHELXD. *Acta Crystallogr. D Biol. Crystallogr.* **58**, 1772–1779.

Schumacher, B., Hofmann, K., Boulton, S., and Gartner, A. (2001). The *C. elegans* homolog of the p53 tumor suppressor is required for DNA damage-induced apoptosis. *Curr. Biol.* **11**, 1722–1727.

Vogelstein, B., Lane, D., and Levine, A.J. (2000). Surfing the p53 network. *Nature* **408**, 307–310.

Waterman, J.L., Shenk, J.L., and Halazonetis, T.D. (1995). The dihedral symmetry of the p53 tetramerization domain mandates a conformational switch upon DNA binding. *EMBO J.* **14**, 512–519.

Zhao, K., Chai, X., Johnston, K., Clements, A., and Marmorstein, R. (2001). Crystal structure of the mouse p53 core DNA-binding domain at 2.7 Å resolution. *J. Biol. Chem.* **276**, 12120–12127.

Accession Numbers

The atomic coordinates and structure factors have been deposited to the Protein Data Bank (PDB ID 1T4W).